DR MINGNAN QU (Orcid ID : 0000-0003-2142-4024)
PROFESSOR CHENGCAI CHU (Orcid ID : 0000-0001-8097-6115)

Article type : Original Article

Alterations in Stomatal Response to Fluctuating Light Increase Biomass and Yield of Rice under Drought conditions

Mingnan Qu[a], Jemaa Essemine[a], Jianlong Xu[b], Guljannat Ablat[a,c], Shahnaz Perveen[a], Hongru Wang[d], Kai Chen[b], Yang Zhao[a], Genyun Chen[a,e,#], Chengcai Chu[d, #], Xinguang Zhu[a, e, #]

[a]National Key Laboratory of Plant Molecular Genetics, CAS Center for Excellence in Molecular Plant Sciences, Shanghai, 200032, China
[b]Institute of Crop Sciences, Chinese Academy of Agricultural Sciences, Beijing, 100081, China
[c]School of Life Sciences, Henan University, Kaifeng 475004, China
[d]State Key Laboratory of Plant Genomics, Institute of Genetics and Developmental Biology, Chinese Academy of Sciences, Beijing, 100101, China
[e]Laboratory of Photosynthesis and Environmental Biology, Shanghai Institute of Plant Physiology and Ecology, Chinese Academy of Sciences, Shanghai, 200032, China

[#]Corresponding authors. X.Z., zhuxg@sippe.ac.cn; C.C., ccchu@genetics.ac.cn; G.C., chenggy@sibs.ac.cn

Running title:

NHX2 affects stomatal dynamics and drought tolerance

This article has been accepted for publication and undergone full peer review but has not been through the copyediting, typesetting, pagination and proofreading process, which may lead to differences between this version and the Version of Record. Please cite this article as doi: 10.1111/TPJ.15004

Key words: Drought tolerance, Stomatal dynamics, OsNHX2, Fluctuating light, Rice. GWAS, Crispr/CAS9

Summary

The acceleration of stomatal closure upon high to low light transition could improve plant water use efficiency (WUE) and drought tolerance. Herein, using genome wide association study (GWAS), we showed that the genetic variation in *OsNHX2* was strongly associated with the changes in τ_{cl}, the time constant of stomatal closure, in 206 rice accessions. *OsNHX2* overexpression in rice resulted in a decrease in τ_{cl} and an increase in biomass, grain yield under drought. Conversely, *OsNHX2* knock-out by CRISPR/CAS9 shows opposite trends for these traits. We further found three haplotypes spanning the *OsNHX2* promoter and CDS regions. Two among them, HapII and HapIII, were found to be associated with a high and low τ_{cl}, respectively. A near isogenic line (NIL, S464) was developed through replacing the genomic region harboring HapII (~10 kb) from MH63 (recipient) rice cultivar by the same sized genomic region containing Hap III from 02428 (donor). Compared to MH63, S464 shows a reduction by 35% in τ_{cl} and an increase by 40% in the grain yield under drought. However, under normal conditions, S464 maintains closely similar grain yield as MH63. The global distribution of the two *OsNHX2* haplotypes is associated with the local precipitation. Taken together, the natural variation in *OsNHX2* could be utilized to manipulate the stomatal dynamics for an improved rice drought tolerance.

Introduction

Drought stress constitutes a major threat for the global food productivity (Boyer, 1982; Timbal, 2004; Bates *et al.*, 2008; Neelin *et al.*, 2006). Many plant morphological features and physiological processes, including root system architectures (Xiong *et al.*, 2006; Yamaguchi and Sharp, 2010), leaf hydraulic conductance and transpiration efficiency are related to plant drought tolerance (Farquhar and Richards, 1984). Extensive efforts are underway to study the molecular mechanisms controlling each of these different traits, with a goal to deliver new approaches to improve crop drought tolerance. The abscisic acid (ABA) metabolism is tightly associated with the drought stress tolerance (Zhu, 2002; Zhu, 2016), which promotes the development of ABA mimic effects compounds such as AMFs and opabactin (Cao *et al.*, 2013; Cao *et al.*, 2017; Vaidya *et al.*, 2019). The ^{13}C carbon isotope signal has been used effectively to improve water use efficiency (WUE) through decreasing the transpiration rates (Richards *et al.*, 2002), which ultimately has led to the development of drought tolerant wheat lines (Richards and Condon, 1993).

Two approaches recently have emerged as potential options to improve crop WUE. The first is to improve mesophyll conductance, g_m (Flexas *et al.*, 2008; Tomas *et al.*, 2013; Xiao *et al.*, 2017; Wang *et al.*, 2018) and the second consists the acceleration in the speed of stomatal closure in response to fluctuating light (Lawson and Blatt, 2014; Qu *et al.*, 2016; Papanatsiou *et al.*, 2019; Lawson and Vialet-Chabrand, 2019). Generally, when water becomes a limiting factor, plants would close stomata to avoid excessive water loss through reducing transpiration and evaporative cooling (Way and Pearcy, 2012; Tricker *et al.*, 2018). Under fluctuating light conditions, the light-response of stomatal conductance (g_s) is often slower than that observed for CO_2 assimilation (A). For instance, A adapts quickly by reaching a new steady-state within several seconds to minutes, whereas it usually takes minutes to hours for g_s to reach a new steady-state (McAusland *et al.*, 2016; Lawson and Vialet-Chabrand, 2019; Flütsch *et al.*, 2020). When leaves are shifted from high to low light, light becomes a limiting factor for the photosynthetic CO_2 uptake (Lawson and Blatt, 2014; McAusland *et al.*, 2016). Under such a condition, maintaining a high g_s would decrease the WUE (Way and Pearcy, 2012). Therefore, a faster speed of stomatal closure, as revealed by the smaller time constant of the stomatal closure during high to low light transition (τ_{cl}), estimated with an exponential regression model, might lead to a higher WUE (Hetherington and Woodward, 2003; Vico *et al.*, 2011). In contrast, a slower stomatal opening might provoke a

decreased light use efficiency (McAusland *et al.*, 2016; Lawson and Vialet-Chabrand, 2019; Flütsch *et al.*, 2020).

The optogenetic manipulation of the stomatal dynamics to increase stomatal response speed promotes indeed the biomass production under drought (Papanatsiou *et al.*, 2019). This optogenetic manipulation involves the expression of a synthetic light-gated K^+-channel BLINK1 in the guard cells to enhance solute fluxes to accelerate the guard cell dynamics (Papanatsiou *et al.*, 2019). The cell-membrane transporters activities for malate, Cl^-, and K^+ were well documented to control the stomatal response speed (Kim *et al.*, 2010; Chen *et al.*, 2012; Wang *et al.*, 2014). Recently, it has been shown also that the starch degradation generates glucose, which is in turn associated with the stomatal opening speed (Flütsch *et al.*, 2020). However, so far, the molecular mechanism governing the variations of stomatal responses remains unknown.

Large variations exist in τ_{cl} among different species, e.g., in some graminoids and forbs species (Vico *et al.*, 2011; Lawson *et al.*, 2012; Drake *et al.*, 2013; McAusland *et al.*, 2016), even within the same species, rice (Qu *et al.*, 2016), under different acclimatory conditions (Matthews *et al.*, 2018). Therefore, identifying the genetic variations in τ_{cl} represents an unexploited opportunity to uncover the promising target molecular markers to promote drought tolerant crop breeding. In the past decades, the genome wide association study (GWAS) has emerged as a powerful tool to elucidate the genetic basis of complex traits. Compared to traditional map-based cloning, GWAS covers much greater allelic diversity and has much higher mapping resolution (Korte and Farlow, 2013). GWAS has been used extensively to dissect the genetic architecture of agronomic traits in different crops, including rice (Huang and Han, 2014), maize (Tian *et al.*, 2011), setaria (Jaiswal *et al.*, 2019), etc. GWAS has also been used to mine new genes controlling g_s (Wang *et al.*, 2020), stomatal size and density (Allwright *et al.*, 2016; Chhetri *et al.*, 2019; McKown *et al.*, 2014), and chlorophyll content (Wang *et al.*, 2015). This demonstrates that GWAS is powerful and reliable to support the genetic studies underlying such physiological traits.

Herein, we applied GWAS on the dataset from two experimental sites to identify candidate genes regulating τ_{cl}. We showed that natural variation of Na^+/H^+ tonoplastic antiporter (*OsNHX2*) was strongly associated with the τ_{cl} in rice. We further identified an elite allelic variation of *OsNHX2*, which can provide high biomass under drought conditions. Importantly, the achieved increase in drought tolerance in rice was not accompanied by any apparent negative impacts on growth and grain yield under normal conditions. Furthermore, the *OsNHX2* allelic variations are tightly associated with the precipitation levels of the origin of different rice accessions. This

implies that the τ_{cl} is under a strong selection pressure. Altogether, this suggests that the *OsNHX2* allelic variation could be utilized as a target molecular marker to breed drought tolerant rice varieties.

Results

Natural variations in τ_{cl}

To study the natural variation of stomatal closure response during high to low light transition, we conducted large-scale stomatal dynamics measurements in 206 minicore rice accessions at two experimental locations, *i.e.*, Beijing (thereafter BJ), and Shanghai (thereafter SH), China. The averaged initial steady-state g_s across the different rice accessions under high light was around ~0.65 mol m^{-2} s^{-1} for both locations (Figure 1a). Upon switching from high to low light, the g_s decreased to about 0.17 and 0.13 mol m^{-2} s^{-1} in around 13 min for BJ and SH, respectively (Figure 1a). We applied an exponential regression model to fit stomatal dynamics during the high to low light switching to estimate τ_{cl} according to Vico *et al.* (2011), following the procedure described in Material and Methods section. The averaged goodness of fit (R^2) across the minicore accessions in BJ and SH was 0.89 and 0.99, respectively (Figure 1a), which indicates that the dynamic model simulated well the stomatal response in rice. An example of a model fitting curve was illustrated in Figure S1. The τ_{cl} values in different accessions follow a normal distribution in BJ but not in SH (Figure 1b). Notably, the mean and median of τ_{cl} in BJ are slightly higher than those in SH (Figure 1b). We found that the ranking of accessions based on τ_{cl} was similar between BJ and SH (Figure 1c), although τ_{cl} differed between BJ and SH experiments (Table S2).

Identification of candidate regulator genes for the stomatal closure speed

We then calculated the SNP heritability of τ_{cl} (h^2_{SNP}) based on 2.3 million SNPs (Wang *et al.*, 2016). The h^2_{SNP} values were 0.35 and 0.11 for BJ and SH, respectively (Figure S2). Using GWAS, we identified 15 SNPs on chromosome 7 (Chr. 7) with a *P*-value less than a defined threshold of 10^{-6} in BJ (Figure 2a and Table S3). The QQ plot shows that the observed $-\log_{10}P$ values were higher than the expected values in the most significant *P*-value range (Figure 2b). A 100-kb region centered on the lead SNP (7m28164743) was selected based on the linkage disequilibrium (LD) decay distance of 50 kb in rice as proposed by (Huang *et al.*, 2010). Thus, 12 candidate genes were identified within the LD block (Figure 2c and Table S4). We further selected 12 rice

accessions with contrasting τ_{cl} values, where 6 accessions characterized by a high τ_{cl} and 6 others with low τ_{cl}. We compared the expression levels of these 12 candidate genes and the values of τ_{cl} between these two groups of accessions (Figure S3a-b). Our results show that, among the 12 identified genes, only *OsNHX2* exhibits significant difference in its expression levels between these two groups ($P < 0.05$) (Figure 2d and Table S5). The accessions with higher τ_{cl} show lower *OsNHX2* expression levels and vice versa (Figure S3a-b). This suggests that *OsNHX2* is a potential negative regulator responsible for τ_{cl}.

Agronomic traits in *OsNHX2* knocked-out and over-expressed lines

The OsNHX2 is an Na^+/H^+ tonoplastic antiporter, belonging to the *NHX* gene family (Barragán *et al.*, 2012). An *OsNHX2* knockout line (*nhx2*) generated with CRISPR/CAS9 technique showed one "T″ allele insertion at the 640th nucleotide position counting from the start codon (ATG), causing an alteration of the amino acids (AA) sequences from the 214th to 250th (Figure 3a,b and Figure S4). Compared to WT, the *nhx2* mutant grown in the field under drought shows a faster stomatal dynamics including closing speed as well as opening speed during low to high light transition (represented by τ_{op}). The *nhx2* mutant shows a 24% decrease in its biomass accumulation under drought (Figure 3c-e and Figure S5a,b). Under drought, there was a reduction in the range of 7~67% for the plant height, tiller number and grain yield in the *nhx2* mutant relative to WT (Figure 3f-g and Table S6), while the growth WUE were higher in WT than in *nhx2* throughout the daytime (8:00 to 18:00) (Figure S6). However, there was no difference in either biomass or τ_{cl} under normal conditions between WT and *nhx2* (Figure 3d, e and Table S6).

The effects of *OsNHX2* knockout on the physiological and morphological traits were further confirmed using three *OsNHX2* homozygous overexpression lines at the T_3 generation (*OsNHX2*-OE) grown under drought in SH. The *OsNHX2*-OE show better performance relative to WT (Figure 3h). The *OsNHX2*-OE lines showed 3~4 folds higher *OsNHX2* expression levels, concurrent with a faster stomatal response speed as indicated by the low τ_{cl} and τ_{op} (Figure 3i, Figure S5c, d and Figure S7a, b). Under drought, these OE lines (*OsNHX2*-OE) exhibited also an increase by 32%, 21% and 45% in biomass, tiller number and grain yield, respectively, compared to WT (Figure 3j-l and Table S6). Besides, no significant difference was recorded in τ_{cl}, biomass and grain yield between WT and *OsNHX2*-OE lines under normal conditions (Figure S8a and Table S6).

We further compared the gene expression levels between *OsNHX2* and its homologous gene, *OsNHX1*, in the *OsNHX2*-OE lines under either normal or drought condition. Our results show that drought caused more than 3-fold increase and about 20% decrease in the expression levels of *OsNHX2* and *OsNHX1*, respectively (Figure S7). Under normal conditions, the expression levels of *OsNHX2* and *OsNHX1* in the *OsNHX2*-OE lines were increased by more than 10 times and decreased by about 60%, respectively (Figure S8b, c). Interestingly, regardless of the growth conditions (drought and normal), the high expression level of *OsNHX2*, in the *OsNHX2*-OE lines, was always accompanied by a low *OsNHX1* expression level (Figure S8d), as reflected by the significant differences, based on the post-hoc statistical test, between the two genes expression levels (Table S7).

The variation of *OsNHX2* haplotypes correlated with τ_{cl} and drought tolerance

Seven significantly associated SNPs were identified in *OsNHX2* gene at a suggestive *P*-value threshold of 10^{-7}. Among them, two SNPs are located in the promoter region (7m28163200 and 7m28164077) and the five other SNPs (7m28164743, 7m28164895, 7m28165064, 7m28167532 and 7m28167928) are situated in the exons (Figure 4a-b and Table S8). To explore the potential INDELs underlying the τ_{cl} trait, a genomic region containing 2,000 bp promoter region upstream of start codon (ATG), 4,924 bp CDS region and 1,304 bp downstream of 3'UTR region from the 12 rice accessions with 6 high and 6 low τ_{cl}, as mentioned above, was re-sequenced. Our sequencing results confirmed the SNP variation in these 12 rice accessions. In addition, we found a single deletion located at 799 bp upstream of ATG (7m28163613). However, this INDEL (deletion) was not associated with the variation in τ_{cl} (Table S8). Besides, we showed that all these SNPs were located within a single LD block and they were genetically strongly inter-correlated between each other (Figure 4c).

We then compared the correlation levels between the *OsNHX2* haplotypes and the τ_{cl} trait. Accordingly, three haplotypes were identified for the seven significant SNPs of *OsNHX2* (Figure 4d). Most accessions with HapII belong to IND subpopulation, while those with HapIII belong to TRJ subpopulation. However, accessions with HapI exist in all the six subpopulations (IND, ARO, AUS, TRJ, TEJ and Admix) (Figure 4e). The τ_{cl} values of accessions with HapIII were relatively lower than those of accessions with HapII (Figure 4f). Out of the 206 rice accessions investigated in this study, 183, 13 and 10 accessions harbor HapI, II and III, respectively (Figure 4f). The τ_{cl} of

accessions with HapI was generally lower than that of HapII and higher than τ_{cl} of HapIII (Figure 4f).

We developed a near isogenic line (NIL), termed S464, of the BC_4F_2 generation derived from two rice parental lines MH63 and 02428, which harbor HapII and HapIII, respectively (Figure S9a). These two lines possess extremely distinct τ_{cl}, where 02428 exhibits low τ_{cl} and MH63 shows high τ_{cl} (Figure S9a). The gene expression level of *OsNHX2* was higher in both S464 and 02428 compared to that in MH63 (Figure S9b). Using 9 molecular markers, listed in Table S1, we narrowed down the recombinant genomic region of S464 which contains *OsNHX2* to ~10 kb (Figure 5a). The drought resistance capability of S464 together with MH63 was evaluated in BJ and SH over two consecutive years. Consistently, our results show that, under drought, S464 exhibited lower τ_{cl} compared to MH63, with a concomitant increase in A, g_s, WUE, plant height, tiller number and biomass. However, under normal conditions, no difference was found between S464 and MH63 across the two years (2018 and 2019) and two locations (BJ and SH) (Figure 5a-f, Figure S10a-f and Table S9).

Correlation of *OsNHX2* haplotypic variations and geoclimate in rice population

It is well known that the long-term stomatal acclimation to an abiotic stress, such as drought, is associated with the anatomical and/or developmental alterations, as shown by the impaired stomatal density, size and index (Hetherington and Woodward, 2003; Xu *et al.*, 2016; Matthews and Lawson, 2019). Since accessions harboring HapII and HapIII showed dramatic differences in τ_{cl} and performed different drought tolerance, we tested whether this haplotypic variation has already been under an artificial selection during the past breeding activities. Specifically, we analyzed the relationship between the two SNP haplotypes and geoclimatic information of the natural habitats for each minicore accession. Our results show that the subgroup containing 13 accessions with HapII and another subgroup containing 10 accessions with HapIII were widely spread in different regions of the world (Figure 6a). In addition, our findings show that there was no significant difference in either the latitudes or longitudes between the two haplotypes subgroups (Figure 6b, c). Interestingly, both the average and the maximum annual precipitations were significantly higher for the natural habitats regions of HapII subgroup than those of HapIII subgroup ($P < 0.05$) (Figure 6d, e). Although there was no difference in the mean temperature between the natural habitat regions of HapII and HapIII subgroups (Figure 6f), the maximum annual temperature was higher in the regions of HapIII subgroup natural habitats than that of

HapII subgroup habitats regions (Figure 6g). This suggests that the stomatal closure speed might have been under an artificial selection during the past rice breeding programs for an increased drought resistance.

Discussion

Increasing the stomatal dynamic is considered as a golden bullet to improve WUE and thereby promote the drought tolerance (Hosy *et al.*, 2003; Flexas *et al.*, 2008; Wang *et al.*, 2018), which was well demonstrated by a synthetic biology study where stomatal dynamics was manipulated in Arabidopsis to gain an increased drought tolerance (Papanatsiou *et al.*, 2019). However, given the large number of involved players, including transporters and enzymes responsible for the regulation of the stomatal dynamics (Jezek and Blatt, 2017; Flütsch *et al.*, 2020) and the complex influences of environmental factors such as light, CO_2 and humidity, on the stomatal dynamics (Buckley, 2005; Araujo *et al.*, 2011), it remains difficult to effectively use this trait (τ_{cl}) in the modern crop breeding programs. Herein, we applied a GWAS approach to identify the molecular markers controlling the variations in τ_{cl}, which could potentially be used in breeding drought resistant rice. In this study, we especially used a global rice minicore diversity panel, which comprises 206 rice accessions and represents around ~85% of the global rice genetic germplasm (Agrama *et al.*, 2009). This rice minicore population was selected base, on one hand, on its sufficient genetic diversity (Agrama *et al.*, 2010) that could ensure optimization of the possibility of identifying new genes responsible for such a trait (Wang *et al.*, 2016), and, on the other hand, on its relatively small accessions number, which enables us measuring the stomatal dynamics easily. Although this is a time-consuming procedure and it remains difficult to study that using the traditional map based cloning approach.

Using GWAS, we identified a rice Na^+/H^+ antiporter (*OsNHX2*), belonging to the *NHX* gene family, to be associated with the time constant of stomatal closure (τ_{cl}) in leaves upon transition from high to low light (Figure 2a, d). The *OsNHX2* belongs to an *NHX* gene family. In Arabidopsis, the *NHX* gene family is divided into two groups, i.e., the vacuolar group which includes *NHX1, NHX2, NHX3* and *NHX4*, and the endosomal group which includes *NHX5* and *NHX6* (McCubbin *et al.*, 2014). The orthologous genes of *OsNHX2* in Arabidopsis (*AtNHX1* and *AtNHX2*) are predominant cation transporters controlling the stomatal opening (Andrés *et al.*, 2014), in addition to the modulation of the plasma membrane pump H^+-ATPase (Yin Wang *et al.*,

2014). The stomatal closure is largely dependent on the vacuolar K^+-release channel TPK1 (Gobert *et al.*, 2007) or the active diffusion of anions through SLAC, a voltage dependent anion channel (Chater and Gray, 2015). An earlier study demonstrated that the *nhx1*×*nhx2* Arabidopsis double mutant shows an impaired stomatal closure (Andrés *et al.*, 2014), which supports a plausible role of *OsNHX2* in the stomatal closure. Here we found that for both *nhx2* mutant and the *OsNHX2*-OE lines, the speeds of stomatal closure and opening were altered simultaneously (Figure 3d, i and Table S6). This is consistent with our earlier observation using the same minicore diversity panel, where we observed a strong positive correlation between τ_{cl} and τ_{op} (Qu *et al.*, 2016). Considering the large number of the involved channels and transporters in the stomatal dynamics regulation and the shared mechanisms of modulating their activities through the membrane potential voltage, pH and Ca^{2+}, it should not be surprising that such a modification affecting anyone of these players could certainly perturb the ion homeostasis in the whole guard cell, causing thereby a simultaneous adjustment and/or modulations in both the stomatal opening and closure kinetics (Jezek and Blatt, 2017).

In Arabidopsis, it has been reported that the *NHX2* is characterized to be associated with the salt tolerance capacity (Fukuda *et al.*, 2011; Teng *et al.*, 2017) and over-expression of *IbNHX2* has been shown to improve drought and salt tolerance in sweat potato, *Ipomoea batatas* L. (Wang *et al.*, 2016). *NHX1* gene was also shown earlier to be involved in drought tolerance in rice (Liu *et al.*, 2010), *Leptochloa fusca* (Rauf *et al.*, 2014), and sweet potato (Zhang *et al.*, 2019). Here, we showed that the over-expression of *OsNHX2* resulted in a faster stomatal closure speed (Figure 3h, i), which ultimately provoked an improved drought tolerance, as reflected by both the higher biomass and grain yield under drought in the OE lines compared to WT (Figure 3j, l and Table S6). Under drought stress concurrently to the increase in the grain yield (Table S6), the *OsNHX2*-OE lines showed also an enhanced g_s by about 23% if compared to WT (Table S6). The maintaining of both higher drought tolerance and higher steady state g_s further confirms the importance of the dynamic responses of g_s in breeding drought-tolerant crops in the field. Improving drought tolerance through engineering stomatal features without deleterious effects on yield under normal condition consists a key target for crop drought tolerant breeding (Caine *et al.*, 2019). This is critical since several currently studied genes controlling drought tolerance towards improving plants survival under extreme drought conditions, have less relevance and output at the agricultural level (Lawlor, 2013).

Interestingly, the *OsNHX2* knockout lines also did not show apparent negative effects on grain yield under normal conditions, which might be attributed to the gene redundancy and the differential gene expression levels between *OsNHX1* and *OsNHX2*. Firstly, there are functional redundancy between *OsNHX2* and its ortholog *OsNHX1* as the case for Arabidopsis (Barragán *et al.*, 2012). Secondly, *OsNHX1* and *OsNHX2* genes show different expression levels under stresses, *e.g.* under salinity and nutrient deficiency (Zeng *et al.*, 2018), and accordingly their expressions might very likely compensate for each other. Consistently, we found that rice lines with lower expression level for *OsNHX2* mostly show a higher expression for *OsNHX1* (Figure S8d).

The identification of molecular markers controlling τ_{cl} could be used in breeding drought tolerant crops. Though many cell membrane transporters and starch degradation metabolism are related to the guard cell dynamics (Kim *et al.*, 2010; Chen *et al.*, 2012; Wang *et al.*, 2014; Flütsch *et al.*, 2020); how the genetic variations of the involved genes could influence the stomatal dynamics has not been studied or reported elsewhere. Here we found that the HapIII of *OsNHX2* represents a promising allele, which confers a fast stomatal response to fluctuating light and an enhanced drought tolerance in rice (Figure 5d; Figure S10 a, d). Overall, this study suggests that the elite allelic variation of *OsNHX2* could be used as a target molecular marker to support future drought tolerant rice breeding strategies, especially in the programs for an upland rice breeding (Bernier *et al.*, 2008). Similarly to rice, *NHX2* controls also the stomatal dynamics in Arabidopsis (Andrés *et al.*, 2014). This implies that the *NHX2* is highly conserved in controlling the stomatal responses to fluctuating light. Therefore, the elite haplotype of *NHX2* may be used in other crops to breed drought tolerant lines. The ability to enhance crop drought tolerance is actually gaining special attention, since with the various available options to improve the photosynthetic efficiency, the expected gain in productivity can only be achieved if a simultaneous improvement in the crop WUE can be realized as well (Long *et al.*, 2015; Wu *et al.*, 2019; Matthews and Lawson, 2019). Notably, the mechanisms by which the different *NHX2* haplotypes control and/or modulate the stomatal movements remain unclear and thus further investigation needs to be done in this context to better explore and decipher the accurate molecular mechanisms standing behind this dynamic paradigm of the puzzling stomatal response to fluctuating light.

Materials and Methods

Rice population and growth conditions

In this study, we used a rice diversity panel containing 206 accessions from the USDA minicore rice germplasm (Agrama *et al.*, 2009). Experiments were conducted in outdoor conditions at two locations, Beijing, BJ (E116°23', N39°54') and Shanghai, SH (E121°13′, N31°02′), China. Given the difference in the weather conditions between the two experimental sites (BJ and SH), the plants were sown on May 20th in SH and May 30th in BJ. Rice seeds from each accession were grown for ~30 days in a soil seed bed first. Then, seedlings were transferred into plastic pots (12 L volume) containing commercial peat soil (Pindstrup Substrate N^{o}. 4) and subsequently kept outdoor in the same condition. Six plants were grown for each rice accessions in two pots (3 plants per pot). The recorded mean air temperature since the sowing date until the stomatal dynamics measurements was around 24.8 (±3.1°C) and 25.5 (±4.4 °C) in BJ and SH, respectively. The relative humidity was around 75%.

Generation of transgenic plants and near isogenic lines

To study the function of *OsNHX2*, an *OsNHX2* mutant was generated using CRISPR/CAS9 by the Biogle company (Hangzhou, China; www.biogle.cn). We designed one single guide RNA (sgRNA) targeting OsNHX2: 5'-GGTCCTCGGCCACCTCCTCG-3'. Through the CRISPR/CAS9 technology, the sgRNA was inserted into the BGK032-DSG vector containing Cas9, which was introduced into an *Agrobacteruim tumefaciens* strain EHA105 and transformed into the wild-type Zhonghua 11 (WT, ZH11) rice cultivar as described previously in details by (Shan *et al.*, 2014). The homozygous lines were sequenced based on the gene specific primers listed in Table S1.

To construct the overexpression vector for *OsNHX2* (*Os07g47100*), its cDNA (primer sequences are listed in Table S1) was amplified from ZH11 and restriction sites (*Bam*HI and *Sac*I) were added and transferred into pCAMBIA 1301 plasmid backbone. This backbone includes a GFP tag (Youbio, China, VT1842) and hygromycin B phosphotransferase (*HPT*) gene driven by 35S promoter (cauliflower mosaic virus). Eventually, the synthesized 35S:*OsNHX2*-GFP constructs were transformed into rice following the earlier reported protocol (Shan *et al.*, 2014) to generate *OsNHX2* over-expression lines (*OsNHX2*-OE).

The T_1 generation of *OsNHX2*-OE lines were planted in a paddy field in Hainan (HN; E110°02′, N18°48′), China, in December 2016. The primers used to detect the positive lines were also listed in Table S1. For each T_1 line of *OsNHX2*-OE, the segregation ratio through *HPT* detection was around 3:1. The T_2 plants from 10 different T_1 lines were grown similarly in a paddy

field in SH, China, in July 2018. Thus, 28 plants were grown for each line. Thereafter, we identified three homozygous OE lines from the T_3 generation for the drought evaluation experiments. Primers used for detecting the *HPT* expression level are also listed in Table S1.

To further elucidate the biological function of the haplotypic variation of *OsNHX2* gene, we developed a near isogenic line (NIL) using two parental lines (MH63 and 02428). MH63 and 02428 possess the HapII and HapIII of *OsNHX2* gene, respectively. The two parental lines (MH63 and 02428) are also characterized by their extremely high and low τ_{cl} values, respectively (Figure S7a). Besides, these two lines (MH63 and 02428) were used as recipient and donor lines, respectively. Then, we selected a NIL, termed S464, in the BC_4F_2 backcross population. S464 harbors the replacement of *OsNHX2* gene in MH63 (recipient) by the entire *OsNHX2* gene from 02428 (donor). The genomic region containing the replaced *OsNHX2* was narrowed down to ~10 kb using 9 INDEL markers as shown in Table S1.

Drought stress treatments

Outdoor drought stress treatments were performed for 206 potted-grown rice accessions at two experimental locations (BJ and SH). Plants were subjected to drought treatments at ~30 days after transplanting (DAT) through controlling soil moisture content as described earlier (Qu *et al.*, 2016). To avoid outdoor precipitation effects, rice plants were sheltered during the raining time. During the drought treatment, plant watering was stopped for a week, during which the soil moisture content across all pots reached ~20%, as monitored by a soil moisture sensor (SM150, Delta-T Devices). Thereafter, we maintained the soil moisture content at around ~30% through re-watering the drought-stressed plants.

To test the potential involvements of *OsNHX2* gene in drought tolerance, the *nhx2* mutant and *OsNHX2*-OE lines were grown under drought and normal conditions in upland and paddy field, respectively, at SH site in 2018. The agronomic traits such as biomass and grain yield were determined for *nhx2* and *OsNHX2*-OE lines under drought and normal conditions. S464 was also grown under the same conditions (upland and paddy field) in SH and HN in two consecutive years (2018 and 2019). Furthermore, to avoid, or at least minimize, the potential boundary effects in our experiments, 36 plants were planted (6×6) with a row space of 20 cm and plants of the same row were spaced by 15 cm. The rice fields were managed according to the standard local agronomic practice as described previously (Qu *et al.*, 2016). Field drought treatment was applied for 15 days by stopping plant watering from 20 DAT. During this period, the soil moisture content decreased

to around 30% as monitored by a moisture sensor SM150 (Delta-T Devices). Plants at 50 DAT were then randomly selected and transferred into pots for gas exchange measurements, morphological traits determinations and photographing.

Geoclimatic information of the minicore population

Geoclimatic data such as latitude and longitude for the origin of each rice accession of the minicore diversity panel were collected from the genetic stock *Oryza sativa* website (http://www.ars.usda.gov/) according to the genetic stock number of each accession as mentioned previously (Qu *et al.*, 2016). Maximum annual temperature, mean and maximum annual precipitations were downloaded from the National Oceanic and Atmospheric Administration (NOAA) database (https://gis.ncdc.noaa.gov/). Overall, the geoclimatic data was collected based on the year during which each accession was released (1914~1997) to determine the original weather conditions for each accession of the minicore population.

Measurements of stomatal closure speed upon high to low light transition

Before stomatal dynamics measurements have been taken, rice plants were transferred to an environment-controlled growth room for about 30 min to ensure stomatal adaptation and a steady-state photosynthesis (Qu *et al.*, 2016). The air temperature of the growth room was maintained at ~27 ^{o}C and the measured photosynthetic photon flux density (PPFD) at the top of the rice canopy was ~1,500 μmol m^{-2} s^{-1}. The middle segment of the top fully expanded leaf of the main tiller was used for stomatal dynamics measurement. The stomatal response upon light switch from high to low light was measured using eight LiCOR-6400XT portable photosynthesis systems (Li-COR, Inc.) between 8:30 am to 16:30 o'clock. We conducted four replicates for each accession. The stomatal dynamics measurements for all rice accessions were completed within 10 days. To minimize the potential complexed effects introduced by the growth stage differences, we measured photosynthetic parameters (including g_s) from accession 1 to 206 sequentially for the first and third replicates, and then we reversed (from accession 206 towards 1) the order of rice accessions for the second and fourth replicates as documented previously (Qu *et al.*, 2017).

The gas exchange measurements for the *nhx2* mutant and the *OsNHX2*-OE lines were performed at ~30th DAT for the plants grown in the field. Gas exchange measurements for the NIL of *OsNHX2* (S464) were carried out at ~40th DAT for the plants grown in the field as well. We

conducted measurements during three continuously sunny days. Usually, fully-expanded leaves were chosen for gas exchange measurements. At least six biological replicates were taken for *nhx2* mutant, *OsNHX2*-OE and NIL.

During the measurements, leaf temperature was maintained at 25 ^{o}C and relative humidity was also controlled to be in the range of 68~ 87%. The reference CO_2 concentration was set to 400 μmol mol^{-1}. During high to low light transition, the leaf was firstly exposed to high light with a PPFD of 1,500 μmol m^{-2} s^{-1} for at least 5 min until it reaches a steady-state photosynthesis. Then, the PPFD was switched to 100 μmol m^{-2} s^{-1} and maintained at this level for ~25 min. After the stabilization of g_s, light was switched back to a PPFD of 1,500 μmol m^{-2} s^{-1}. Measurement of the fluctuating light response of g_s was described previously (Qu *et al.*, 2016). For data analysis, we fitted the stomatal dynamics data with a first order exponential decay curve using MATLAB software, version R2010a (Mathworks Inc., Natick, MA, USA) to estimate τ_{cl} as reported in (Vico *et al.*, 2011) using the following equation:

$$g_{(t)}=g^*_{(\varphi)}+[g_0-g^*_{(\varphi)}]\times\exp(-t/\tau_g)$$

where τ_g reflects different values depending on whether the g_s endured a sudden increase (τ_{op}) or decrease (τ_{cl}) in the light levels. In this study, we performed GWAS on τ_{cl}, which represents the time constant for stomatal closure upon high to low light transition. The time scale used to estimate τ_{cl} covers 63% of the difference between the initial g_s values and the asymptotic g_s values according to Vico *et al.*, (2011). The goodness of fit obtained from the exponential regression during stomatal closing phase across the minicore rice population in the two experimental locations (BJ and SH) was in the range of 0.76 to 0.98. This corroborates the accuracy and goodness of our exponential fitting procedure. The WUE (A/g_s) was calculated based on the measured A and g_s under high light before light is switched to 100 μmol m^{-2} s^{-1}.

Identification of the candidate gene using GWAS as a powerful approach

The whole-genome of the rice accessions used in this study were earlier genotyped (Wang *et al.*, 2016). In total, 2.3 million biallelic SNPs with a minor allele frequency (MAF) ≥ 5% were used in the association mapping. The values of τ_{cl} were first normalized with Quantile-Quantile (QQ) plots *norm* function of the R software (version 3.2.1). Then, we performed GWAS with a linear mixed model (LMM) implemented in GEMMA software (Wang *et al.*, 2016).

To correct the population structure and reduce false positive rates, we performed a principal component analysis (PCA) on the SNP matrix of minicore population and used the first 4 principle

components as covariates in the GWAS analysis following Wang *et al.* (2016). We used, thereafter, a permutation strategy to define the significant SNPs at the genomic level. Using 200 permutations, we determined a *P*-value of 10^{-6} as the genome-wide significant threshold as proposed earlier (Hamdani *et al.*, 2019). A linkage disequilibrium (LD) analysis was also conducted with the Haploview software (version 4.2) to investigate the relatedness degree of the candidate genes to the lead SNP. The LD blocks were generated when the upper 95% confidence bounds of r^2 value exceeds 0.98 and the lower bounds exceeds 0.70 (Gabriel *et al.*, 2002). The genes identified in the LD block were selected as potential candidate genes that might control τ_{cl}.

Estimation of SNP heritability

The SNP heritability represents the proportion of phenotypic variance explained by SNPs (Speed *et al.*, 2017). We estimated the SNP heritability of the stomatal dynamics using the GCTA software (version 1.11.2 beta) based on the Restricted Maximum Likelihood method. A Log Likelihood Test (LRT) was used to calculate the *P*-value of SNP heritability according to the GCTA software manual.

Screening the candidate genes using gene expression analysis

We further screened the candidate genes potentially controlling the τ_{cl} trait based on the association of transcription level and τ_{cl}. In this regard, we selected 12 accessions with contrasting τ_{cl} values (6 low and 6 high) from the experiments performed at both locations (BJ and SH). The selected accessions are listed in Table S4. We further conducted quantitative real-time polymerase chain reaction (qRT-PCR) analysis (ABI StepOnePlus, Applied Biosystems Co., Ltd., USA) for the candidate genes previously identified by LD-block analysis. For qRT-PCR analysis, samples were collected from the top fully expanded leaves at 30 DAT from plants grown in the growth chamber. The total RNA was extracted using ambion PureLink™ RNA mini kit according to manufacturer's instruction.

Subsequently, two micrograms of the total RNA were reversely transcribed to cDNA with SuperScript VILO cDNA Synthesis Kit (Invitrogen Life Technologies, http://www.invitrogen.com). The qRT-PCR analysis was performed using SYBR Green PCR Master Mix (Applied Biosystems, USA) with cDNA as a template and following the cycling steps: 95°C for 10 s, 55°C for 20 s, and 72°C for 20 s. The specific primers for qRT-PCR were designed using Primer Prime Plus 5 Software Version 3.0 (Applied Biosystems, USA). The primer sequences are

displayed in the Table S1. The relative expression of gene against Actin (the housekeeping gene) was calculated as follows: $2^{-\Delta\Delta CT}$ (ΔCT = CT, gene of interest−CT, Actin) (Livak and Schmittgen, 2001). Six biological replicates and three technical replicates for each biological replicate were performed for each gene.

Data and materials availability: All data is available in the manuscript or the Supporting Information. Thus, this document includes 10 Figures and 9 Tables as supplementary materials.

Acknowledgements

This work was supported by Chinese Strategic Leading project category B (XDB27020105), National Natural Science Foundation of China (31700201) and Sailing Project, Shanghai Municipal Science and Technology Commission, China (17YF1421800), Chinese Strategic Leading project category A (XDA08020301).

Author contributions: Conceptualization, Y.Z., X.Z., C.C.; Methodology, M.Q., H.W., S.P., G.Y.; Investigation, M.Q., S.P., K.C., G.A., K.C.; Writing, M.Q., X.Z, J.E.; Funding Acquisition, X.Z. Resources, C.C, J.X.; Supervision, X.Z.

Conflict of interest: The authors have no competing of interests to declare.

Short supporting materials legends:

Table S1. List of primers used in this study.
Table S2. Two way *ANOVA* and post-hoc test from Tukey multiple comparisons on the speed of stomatal closure in response to the effects of growth environments and rice subpopulations.
Table S3. List of SNPs above the threshold of significant level and their corresponding *P*-values.
Table S4. List and annotation of candidate genes surrounding the lead SNP within 100 kb genomic region in rice.
Table S5. qPCR results for candidate genes using two rice subgroups with contrasting stomatal dynamics phenotypes (low or high τ_{cl}).
Table S6. Morphological and physiological traits across *OsNHX2* overexpression lines and its knockout lines grown under control and drought conditions in the field (Shanghai, SH).

Table S7. Two way *ANOVA* and post-hoc test from Tukey multiple comparisons on the gene expression levels in response to two *NHX* genes (*NHX1* and *NHX2*) and three overexpression lines.

Table S8. SNP variation analysis of *OsNHX2* gene in 12 rice accessions characterized by their contrasting stomatal dynamics phenotypes (low or high τ_{cl}).

Table S9. Physiological and morphological traits in MH63 and *OsNHX* near isogeneic line (NIL-S464) evaluated under control and drought condition in two field locations (Shanghai, SH and Hainan, HN) over two years.

Figure S1. A representative fitting figure using exponential model to depict the stomatal response to fluctuating light.

Figure S2. The SNP-based heritability of τ_{cl} under two growth conditions (Beijing, BJ and Shanghai, SH).

Figure S3. Time-constant of the stomatal closure (τ_{cl}) and gene expression of *OsNHX2*.

Figure S4. Sequencing results of homozygous CRISPR-edited *OsNHX2* knock-out lines.

Figure S5. Comparison of stomatal dynamics in WT and *OsNHX2* overexpressed (OE) lines in field under drought conditions.

Figure S6. Response of water use efficiency (WUE) to diurnal changes in WT and *nhx2* grown in field under drought conditions.

Figure S7. Gene expression of *OsNHX2* and *OsNHX1* in *NHX2-OE* lines of T_3 generation in field under drought conditions.

Figure S8. Performance of *NHX2-OE* lines in field under normal conditions.

Figure S9. Development of *OsNHX2* near isogenic line (NIL).

Figure S10. The time constants of the stomatal closure (τ_{cl}) and grain yield for MH63 and an *OsNHX2*-NIL (S464) grown in the field under either control or drought stress condition.

References

Agrama, H.A., Yan, W., Jia, M., Fjellstrom, R. and McClung, A.M. (2010) Genetic structure associated with diversity and geographic distribution in the USDA rice world collection. *Nat. Sci.*, **02**, 247–291.

Agrama, H.A., Yan, W.G., Lee, F., Robert, F., Chen, M.H., Jia, M. and McClung, A. (2009) Genetic assessment of a mini-core subset developed from the USDA rice genebank. *Crop Sci.*, **49**, 1336–1346.

Allwright, M.R., Payne, A., Emiliani, G., et al. (2016) Biomass traits and candidate genes for bioenergy revealed through association genetics in coppiced European Populus nigra (L.). *Biotechnol. Biofuels*, **9**, 195.

Andrés, Z., Pérez-Hormaeche, J., Leidi, E.O., et al. (2014) Control of vacuolar dynamics and regulation of stomatal aperture by tonoplast potassium uptake. *Proc. Natl. Acad. Sci. U. S. A.*, **111**.

Araujo, W.L., Fernie, A.R. and Nunes-Nesi, A. (2011) Control of stomatal aperture: a renaissance of the old guard. *Plant Signal. Behav.*, **6**, 1305–1311.

Barragán, V., Leidi, E.O., Andrés, Z., Rubio, L., Luca, A. de, Fernández, J.A., Cubero, B. and Pardo, J.M. (2012) Ion exchangers NHX1 and NHX2 mediate active potassium uptake into vacuoles to regulate cell turgor and stomatal function in arabidopsis. *Plant Cell*, **24**, 1127–1142.

Bates, B.C., Hope, P., Ryan, B., Smith, I. and Charles, S. (2008) Key findings from the Indian Ocean Climate Initiative and their impact on policy development in Australia. *Clim. Change*, **89**, 339–354.

Bernier, J., Atlin, G.N., Serraj, R., Kumar, A. and Spaner, D. (2008) Breeding upland rice for drought resistance. *J. Sci. Food Agric.*, **88**, 927–939.

Boyer, J.S. (1982) Plant productivity and environment. *Science*, **218**, 443–448.

Buckley, T. (2005) The control of stomata by water balance. *New Phytol.*, **168**, 275–292.

Caine, R.S., Yin, X., Sloan, J., et al. (2019) Rice with reduced stomatal density conserves water and has improved drought tolerance under future climate conditions. *New Phytol.*, **221**, 371–384.

Cao, M.-J., Zhang, Y.-L., Liu, X., et al. (2017) Combining chemical and genetic approaches to increase drought resistance in plants. *Nat. Commun.*, **8**, 1183.

Cao, M., Liu, X., Zhang, Y., et al. (2013) An ABA-mimicking ligand that reduces water loss and promotes drought resistance in plants. *Cell Res.*, **23**, 1043–1054.

Chater, C. and Gray, J. (2015) Stomatal closure: The old guard takes up the SLAC. *Curr. Biol.*, **25**, R271-3.

Chen, Z.H., Hills, A., Bätz, U., Amtmann, A., Lew, V.L. and Blatt, M.R. (2012) Systems dynamic modeling of the stomatal guard cell predicts emergent behaviors in transport, signaling, and volume control. *Plant Physiol.*, **159**, 1235–1251.

Chhetri, H.B., Macaya-Sanz, D., Kainer, D., et al. (2019) Multitrait genome-wide association analysis of Populus trichocarpa identifies key polymorphisms controlling morphological and physiological traits. *New Phytol.*, **223**, 293–309.

Drake, P.L., Froend, R.H. and Franks, P.J. (2013) Smaller, faster stomata: Scaling of stomatal size, rate of response, and stomatal conductance. *J. Exp. Bot.*, **64**, 495–505.

Farquhar, G.D. and Richards, R.A. (1984) Isotopic composition of plant carbon correlates with water-use efficiency of wheat genotypes. *Funct. Plant Biol.*, **11**, 539–552.

Flexas, J., Ribas-Carbo, M., Diaz-Espejo, A., Galmes, J. and Medrano, H. (2008) Mesophyll conductance to CO_2: current knowledge and future prospects. *Plant. Cell Environ.*, **31**, 602–621.

Flütsch, S., Wang, Y., Takemiya, A., et al. (2020) Guard cell starch degradation yields glucose for rapid stomatal opening in Arabidopsis. *Plant Cell*, tpc.00802.2018.

Fukuda, A., Nakamura, A., Hara, N., Toki, S. and Tanaka, Y. (2011) Molecular and functional analyses of rice NHX-type Na^+/H^+ antiporter genes. *Planta*, **233**, 175–188.

Gabriel, S.B., Schaffner, S.F., Nguyen, H., et al. (2002) The structure of haplotype blocks in the human genome. *Science*, **296**, 2225–2229.

Gobert, A., Isayenkov, S., Voelker, C., Czempinski, K. and Maathuis, F.J.M. (2007) The two-pore channel *TPK1* gene encodes the vacuolar K^+ conductance and plays a role in K^+ homeostasis. *Proc. Natl. Acad. Sci.*, **104**, 10726 LP – 10731.

Hamdani, S., Wang, H., Zheng, G., et al. (2019) Genome-wide association study identifies variation of glucosidase being linked to natural variation of the maximal quantum yield of photosystem II. *Physiol. Plant.*, **166**.

Hetherington, A.M. and Woodward, F.I. (2003) The role of stomata in sensing and driving environmental change. *Nature*, **424**, 901–908.

Hosy, E., Vavasseur, A., Mouline, K., et al. (2003) The Arabidopsis outward K+ channel GORK is involved in regulation of stomatal movements and plant transpiration. *Proc. Natl. Acad. Sci. U. S. A.*, **100**, 5549–5554.

Huang, X. and Han, B. (2014) Natural variations and genome-wide association studies in crop plants. *Annu. Rev. Plant Biol.*, **65**, 531–551.

Huang, X., Wei, X., Sang, T., et al. (2010) Genome-wide asociation studies of 14 agronomic traits in rice landraces. *Nat. Genet.*, **42**, 961–967.

Jaiswal, V., Gupta, S., Gahlaut, V., Muthamilarasan, M., Bandyopadhyay, T., Ramchiary, N. and Prasad, M. (2019) Genome-wide association study of major agronomic traits in foxtail millet (*Setaria italica* L.) using ddRAD sequencing. *Sci. Rep.*, **9**, 5020.

Jezek, M. and Blatt, M.R. (2017) The Membrane Transport System of the Guard Cell and Its Integration for Stomatal Dynamics. *Plant Physiol.*, **174**, 487–519.

Kim, T.-H., Böhmer, M., Hu, H., Nishimura, N. and Schroeder, J.I. (2010) Guard cell signal transduction network: advances in understanding abscisic acid, CO_2, and Ca^{2+} signaling. *Annu. Rev. Plant Biol.*, **61**, 561–591.

Korte, A. and Farlow, A. (2013) The advantages and limitations of trait analysis with GWAS: A review. *Plant Methods*, **9**, 1.

Lawlor, D.W. (2013) Genetic engineering to improve plant performance under drought: physiological evaluation of achievements, limitations, and possibilities. *J. Exp. Bot.*, **64**, 83–108.

Lawson, T. and Blatt, M.R. (2014) Stomatal size, speed, and responsiveness impact on photosynthesis and water use efficiency. *Plant Physiol.*, **164**, 1556–1570.

Lawson, T., Kramer, D.M. and Raines, C.A. (2012) Improving yield by exploiting mechanisms underlying natural variation of photosynthesis. *Curr. Opin. Biotechnol.*, **23**, 215–220.

Lawson, T. and Vialet-Chabrand, S. (2019) Speedy stomata, photosynthesis and plant water use efficiency. *New Phytol.*, **221**, 93–98.

Liu, S., Zheng, L., Xue, Y., Zhang, Q., Wang, L. and Shou, H. (2010) Overexpression of OsVP1 and OsNHX1 increases tolerance to drought and salinity in rice. *J. Plant Biol.*, **53**, 444–452.

Livak, K.J. and Schmittgen, T.D. (2001) Analysis of relative gene expression data using real-time quantitative PCR and the 2(-Delta Delta C(T)) Method. *Methods*, **25**, 402–408.

Long, S.P., Marshall-Colon, A. and Zhu, X.G. (2015) Meeting the global food demand of the future by engineering crop photosynthesis and yield potential. *Cell*, **161**, 56–66.

Matthews, J.S.A. and Lawson, T. (2019) Climate change and stomatal physiology. *Annu. Plant Rev.*, **2**, 713–752.

Matthews, J.S.A., Vialet-Chabrand, S. and Lawson, T. (2018) Acclimation to fluctuating light impacts the rapidity of response and diurnal rhythm of stomatal conductance. *Plant Physiol.*, **176**, 1939 LP – 1951.

McAusland, L., Vialet-Chabrand, S., Davey, P., Baker, N.R., Brendel, O. and Lawson, T. (2016) Effects of kinetics of light-induced stomatal responses on photosynthesis and water-use efficiency. *New Phytol.*, **211**, 1209–1220.

McCubbin, T., Bassil, E., Zhang, S. and Blumwald, E. (2014) Vacuolar Na^+/H^+ NHX-type antiporters are required for cellular K^+ homeostasis, microtubule organization and directional root growth. *Plants*, **3**, 409–426.

McKown, A.D., Guy, R.D., Quamme, L., et al. (2014) Association genetics, geography and ecophysiology link stomatal patterning in Populus trichocarpa with carbon gain and disease resistance trade-offs. *Mol. Ecol.*, **23**, 5771–5790.

Neelin, J.D., Münnich, M., Su, H., Meyerson, J.E. and Holloway, C.E. (2006) Tropical drying trends in global warming models and observations. *Proc. Natl. Acad. Sci.*, **103**, 6110 LP – 6115.

Papanatsiou, M., Petersen, J., Henderson, L., Wang, Y., Christie, J.M. and Blatt, M.R. (2019) Optogenetic manipulation of stomatal kinetics improves carbon assimilation, water use, and growth. *Science*, **363**, 1456–1459.

Qu, M., Hamdani, S., Li, W., et al. (2016) Rapid stomatal response to fluctuating light: An under-explored mechanism to improve drought tolerance in rice. *Funct. Plant Biol.*, **43**, 727–738.

Qu, M., Zheng, G., Hamdani, S., Essemine, J., Song, Q., Wang, H., Chu, C., Sirault, X. and Zhu, X.G. (2017) Leaf photosynthetic parameters related to biomass accumulation in a global rice diversity survey. *Plant Physiol.*, **175**, 248–258.

Rauf, M., Shahzad, K., Ali, R., Ahmad, M., Habib, I., Mansoor, S., Berkowitz, G.A. and Saeed, N.A. (2014) Cloning and characterization of Na^+/H^+ antiporter (LfNHX1) gene from a halophyte grass Leptochloa fusca for drought and salt tolerance. *Mol. Biol. Rep.*, **41**, 1669–1682.

Richards, R.A. and Condon, A.G. (1993) 29 - Challenges ahead in using carbon isotope discrimination in plant-breeding programs. In J. R. Ehleringer, A. E. Hall, and G. D. B. T.-S. I. and P. C. R. Farquhar, eds. San Diego: Academic Press, pp. 451–462.

Richards, R.A., Rebetzke, G.J., Condon, A.G. and Herwaarden, A.F. van (2002) Breeding opportunities for increasing the efficiency of water use and crop yield in temperate cereals. *Crop Sci.*, **42**, 111–121.

Shan, Q., Wang, Y., Li, J. and Gao, C. (2014) Genome editing in rice and wheat using the CRISPR/Cas system. *Nat. Protoc.*, **9**, 2395–2410.

Speed, D., Cai, N., Johnson, M.R., Nejentsev, S. and Balding, D.J. (2017) Reevaluation of SNP heritability in complex human traits. *Nat. Genet.*, **49**, 986–992.

Teng, X.-X., Cao, W.-L., Lan, H.-X., Tang, H.-J., Bao, Y.-M. and Zhang, H.-S. (2017) OsNHX2, an Na^+/H^+ antiporter gene, can enhance salt tolerance in rice plants through more effective accumulation of toxic Na^+ in leaf mesophyll and bundle sheath cells. *Acta Physiol. Plant.*, **39**, 113.

Tian, F., Bradbury, P.J., Brown, P.J., et al. (2011) Genome-wide association study of leaf architecture in the maize nested association mapping population. *Nat. Genet.*, **43**, 159–162.

Timbal, B. (2004) South West Australia past and future rainfall trends. *Clim. Res. - Clim. RES*, **26**, 233–249.

Tomas, M., Flexas, J., Copolovici, L., et al. (2013) Importance of leaf anatomy in determining mesophyll diffusion conductance to CO_2 across species: quantitative limitations and scaling up by models. *J. Exp. Bot.*, **64**, 2269–2281.

Tricker, P.J., ElHabti, A., Schmidt, J. and Fleury, D. (2018) The physiological and genetic basis of combined drought and heat tolerance in wheat. *J. Exp. Bot.*, **69**, 3195–3210.

Vaidya, A.S., Helander, J.D.M., Peterson, F.C., et al. (2019) Dynamic control of plant water use using designed ABA receptor agonists. *Science*, **366**.

Vico, G., Manzoni, S., Palmroth, S. and Katul, G. (2011) Effects of stomatal delays on the economics of leaf gas exchange under intermittent light regimes. *New Phytol.*, **192**, 640–652.

Wang, B., Zhai, H., He, S., Zhang, H., Ren, Z., Zhang, D. and Liu, Q. (2016) A vacuolar Na^+/H^+ antiporter gene, IbNHX2, enhances salt and drought tolerance in transgenic sweetpotato. *Sci. Hortic. (Amsterdam).*, **201**, 153–166.

Wang, H., Xu, X., Vieira, F.G., Xiao, Y., Li, Z., Wang, J., Nielsen, R. and Chu, C. (2016) The power of inbreeding: NGS-based GWAS of rice reveals convergent evolution during rice domestication. *Mol. Plant*, **9**, 975–985.

Wang, Hills, A. and Blatt, M.R. (2014) Systems analysis of guard cell membrane transport for enhanced stomatal dynamics and water use efficiency. *Plant Physiol.*, **164**, 1593 LP – 1599.

Wang, L., Yang, Y., Zhang, S., Che, Z., Yuan, W. and Yu, D. (2020) GWAS reveals two novel loci for photosynthesis-related traits in soybean. *Mol. Genet. Genomics*, **295**, 705–716.

Wang, Q., Xie, W., Xing, H., et al. (2015) Genetic architecture of natural variation in rice chlorophyll content revealed by a genome-wide association study. *Mol. Plant*, **8**, 946–957.

Wang, X., Du, T., Huang, J., Peng, S. and Xiong, D. (2018) Leaf hydraulic vulnerability triggers the decline in stomatal and mesophyll conductance during drought in rice. *J. Exp. Bot.*, **69**, 4033–4045.

Wang, Yizhou, Hills, A. and Blatt, M.R. (2014) Systems analysis of guard cell membrane transport for enhanced stomatal dynamics and water use efficiency. *Plant Physiol.*, **164**, 1593–1599.

Wang, Yin, Noguchi, K., Ono, N., Inoue, S., Terashima, I. and Kinoshita, T. (2014) Overexpression of plasma membrane H^+-ATPase in guard cells promotes light-induced stomatal opening and enhances plant growth. *Proc. Natl. Acad. Sci. U. S. A.*, **111**, 533–538.

Way, D.A. and Pearcy, R.W. (2012) Sunflecks in trees and forests: from photosynthetic physiology to global change biology. *Tree Physiol.*, **32**, 1066–1081.

Wu, A., Hammer, G.L., Doherty, A., Caemmerer, S. von and Farquhar, G.D. (2019) Quantifying impacts of enhancing photosynthesis on crop yield. *Nat. Plants*, **5**, 380–388.

Xiao, Y., Chang, T., Song, Q., et al. (2017) ePlant for quantitative and predictive plant science research in the big data era—Lay the foundation for the future model guided crop breeding, engineering and agronomy. *Quant. Biol.*, **5**, 260–271.

Xiong, L., Wang, R.-G., Mao, G. and Koczan, J.M. (2006) Identification of drought tolerance determinants by genetic analysis of root response to drought stress and abscisic Acid. *Plant Physiol.*, **142**, 1065–1074.

Yamaguchi, M. and Sharp, R.E. (2010) Complexity and coordination of root growth at low water potentials: recent advances from transcriptomic and proteomic analyses. *Plant. Cell Environ.*, **33**, 590–603.

Zeng, Y., Li, Q., Wang, H., Zhang, J., Du, J., Feng, H., Blumwald, E., Yu, L. and Xu, G. (2018) Two NHX-type transporters from *Helianthus tuberosus* improve the tolerance of rice to salinity and nutrient deficiency stress. *Plant Biotechnol. J.*, **16**, 310–321.

Zhang, Y., Deng, G., Fan, W., Yuan, L., Wang, H. and Zhang, P. (2019) NHX1 and eIF4A1-stacked transgenic sweetpotato shows enhanced tolerance to drought stress. *Plant Cell Rep.*, **38**, 1427–1438.

Zhu, J.-K. (2016) Abiotic stress signaling and responses in plants. *Cell*, **167**, 313–324.

Zhu, J.-K. (2002) Salt and drought stress signal transduction in plants. *Annu. Rev. Plant Biol.*, **53**, 247–273.

Figures legends

Figure 1. Evaluation of stomatal response to fluctuating light in rice population at two growth locations. (a) Stomatal responses during light switch (high-low-high) in a rice minicore population (206 accessions) at two growth sites; Beijing, BJ (E116°23', N39°54') and Shanghai, SH (E121°13′, N31°02′), China. A stomatal dynamic model was employed to derive the time constant of stomatal closure speed (τ_{cl}) during the light switch experiment. The horizontal double-headed arrow displays the time scale used for the simulation model. Goodness of fit (R^2), degree of confidence to which our results can be relied, was 0.89 and 0.80 for BJ and SH, respectively. (b) Distribution of τ_{cl} determined at two experimental locations (BJ and SH). (c) Comparison on ranking different subpopulations in minicore panel with distinct measured τ_{cl} between two growth locations (BJ and SH). For panel (a), each curve represents the average for 206 rice accessions with 4 replicates for each accession (±SE).

Figure 2. Identification of *OsNHX2* as a candidate gene controlling the speed of stomatal closure during high to low light transition. (a) Manhattan plot showing the genome-wide association study (GWAS) on τ_{cl} measured at BJ on 206 rice accessions. The dotted cutoff horizontal line represents the threshold *P*-value, estimated based on 2.3 million genomic SNPs of the rice minicore diversity panel. (b) Quantile-Quantile (QQ)-plot representing the statistical significance of measured versus predicted results using GWAS on τ_{cl} measured at BJ. (c) Candidate genes in the genomic region surrounding the highest associated SNP. A ±50 kb genomic region surrounding the highest associated SNP (7m28164743) was selected to identify the candidate genes. (d) Relative expression levels of the candidate genes in accessions with low τ_{cl} or high τ_{cl} (12 accessions). More details about the rice accessions used for qRT-PCR are available in Table S1. Six biological replicates were conducted for qRT-PCR analysis. For panel (d), the results are shown as the mean values (±SE).

Figure 3. *OsNHX2* regulates the speed of stomatal closure during high to low light transition and subsequently influences drought tolerance in field conditions. (a) The targeted-position by the gRNA of CRISPR/CAS9 system in *nhx2* rice mutant. The gRNA sequence is 5"-GGTCCTCGGCCACCTCCTCG-3". (b) Alterations of the amino acids (AAs) sequence due to the mutation introduced by the CRISPR/CAS9. Pos. of AA represents the position of amino acid.

Unchanged AAs were shown in bold. "-" stands for stop codon. (c) Photos of WT (ZH11) and *nhx2* grown in the field under both normal and drought conditions at SH. Randomly selected plants for both normal and drought stress were transferred to pots for photographing at ~40th DAT.. (d-g) τ_{cl}, biomass, tiller number and grain yield for WT and *nhx2* under normal and drought conditions. (h) Photos of WT (ZH11) and three *OsNHX2*-OE lines grown under drought in the field in SH. Randomly selected plants grown under drought condition were transferred to pots for photographing at ~50th DAT. (i-l) τ_{cl}, biomass, tiller number and grain yield for WT and *OsNHX2*-OE lines grown under drought. White vertical bar in the photos of panels (c) and (h) represents the scaling bar of 10 cm length. For panels (d) and (i), each bar data represents the mean of 6 different replicates (±SE). For panels (e-f and j-k), each bar data is the average of 20 different replicates (±SE).

Figure 4. A SNP variation in *OsNHX2* strongly associated with the stomatal dynamics. (a) Zoom-out of the Manhattan plot against 5 kb genomic region centering the promoter and CDS regions of *OsNHX2*. The seven significantly associated SNPs with τ_{cl} were highlighted in red. (b) Genomic positions of the seven SNPs relative to the start codon (ATG) in the *OsNHX2* gene. (c) Correlation between the seven SNPs displayed in the linkage disequilibrium (LD) block built with the haploview software (version 4.1). (d) AA changes due to the SNPs were classified into three *OsNHX2* haplotypes. The corresponding AAs are shown between brackets. Dis. to ATG represents the distance of each SNP to ATG (start codon). (e) The distribution of *OsNHX2* haplotypes in different rice subpopulations. (f) The distribution of τ_{cl} in three SNP haplotypes. The number of accessions for each haplotype was indicated in brackets. In panel (b), ″P″ stands for promoter.

Figure 5. Field performance of *OsNHX2*-NIL under drought condition in two experimental sites carried out on two consecutive years. (a) Photos of *OsNHX2*-NIL (S464), MH63 and 02428 grown at SH in 2018. Randomly chosen plants were transferred to pots for photographing at about 50th DAT. The *OsNHX2*-NIL (S464) was created using MH63 as a recipient line while 02428 as a recurrent (donor) parent. S464 is a BC_4F_2 offspring which includes an *OsNHX2*-containing ~10 kb genomic region from 02428. The nine primer pairs designed as indicated in orange vertical lines at different positions of the S464 genomic region are listed in Table S1. (b-c) τ_{cl} and grain yields in S464, MH63 and 02428. (d) Photos of S464 and MH63 grown at SH in 2019. Randomly selected plants were transferred to pots for photographing at ~ 50th DAT. (e-f) The τ_{cl} and grain yield in S464 and MH63. In panel (b), different alphabet letters represent the

significant difference at the *P*-value < 0.05, which was calculated based on one-way *ANOVA*. For the τ_{cl} of panels (b) and (e), each bar data represents the mean of 6 different replicates (±SE). White vertical bars in the photos of panels (a) and (d) represent the scaling bar of 10 cm length. The values of grain yield in panel (c) and (f) were determined from six random blocks in the field and from each block at least 30 replicates have been taken.

Figure 6. Relationship between SNP haplotypes and geoclimate of the original regions of the rice minicore population. (a) World-wide distribution of the two SNP haplotypes (HapII and HapIII) of *OsNHX2*. The information for the global mean precipitation for the year 2011 was obtained from mecometer website (http://mecometer.com/topic/average-yearly-precipitation/). (b-g) Latitude and longitude, mean and maximum precipitation (mm $year^{-1}$), mean and maximum annual temperature in the regions from where accessions harboring the two SNP haplotypes (HapII and HapIII) were originally collected. The information about precipitation and maximum annual temperature of the minicore population was collected from NOAA database (https://gis.ncdc.noaa.gov). Adjacent *P*-values to the bars of histograms were calculated based on *t*-test.

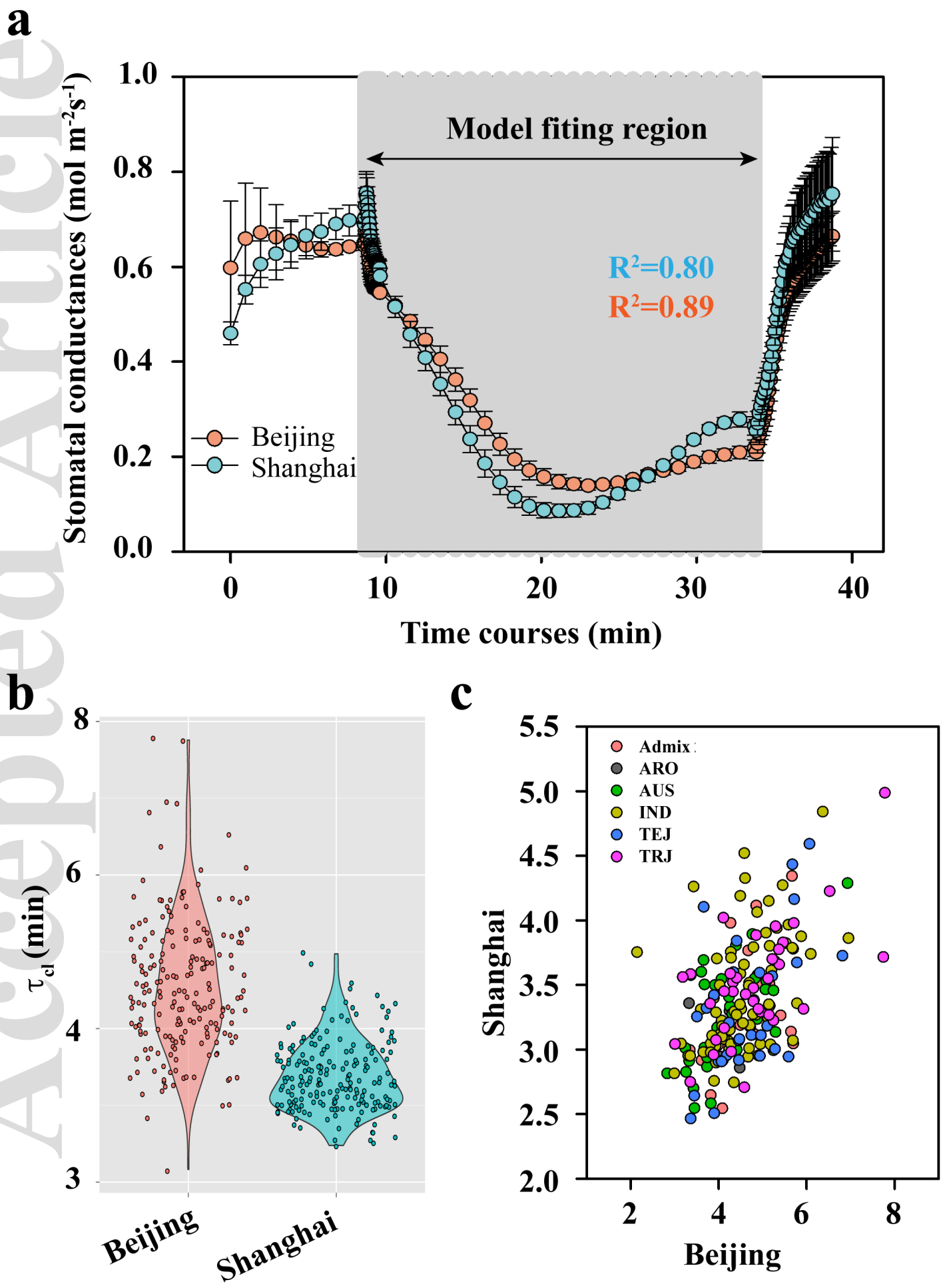

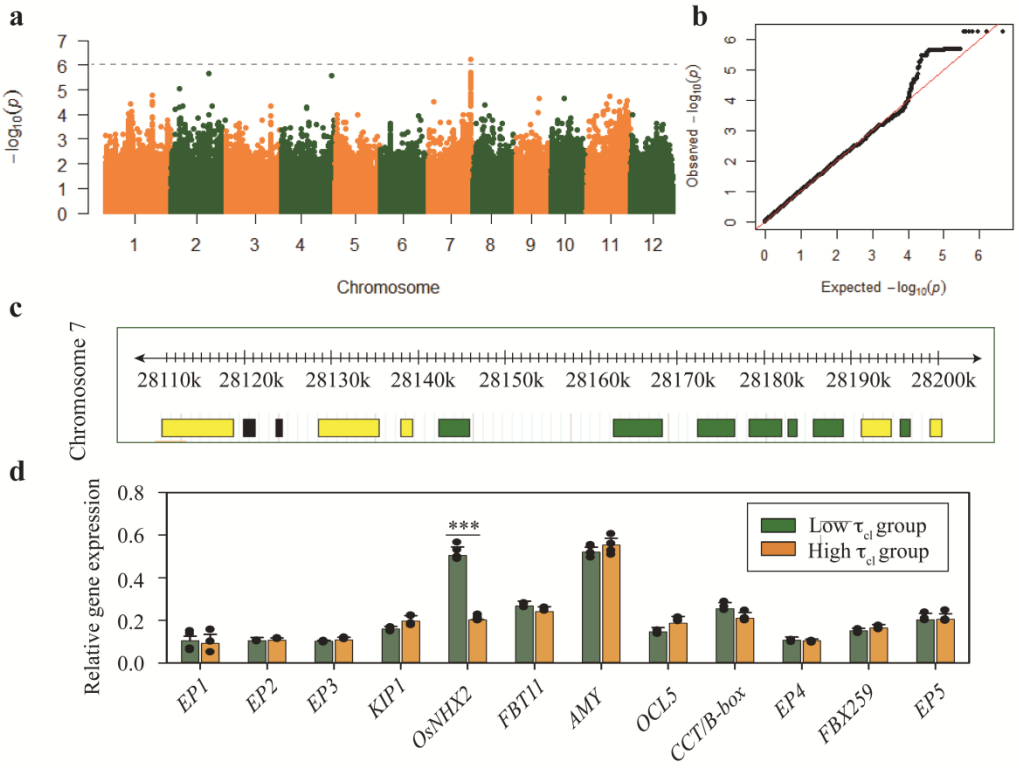

tpj_15004_f2.tif

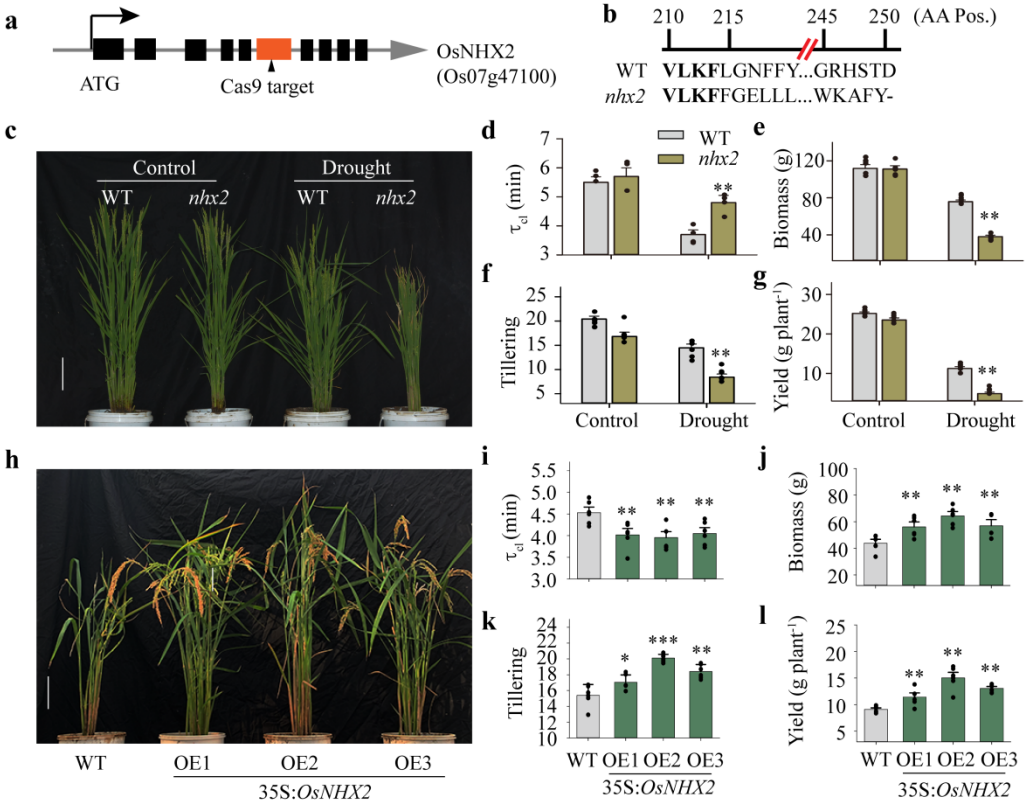

tpj_15004_f3.tif

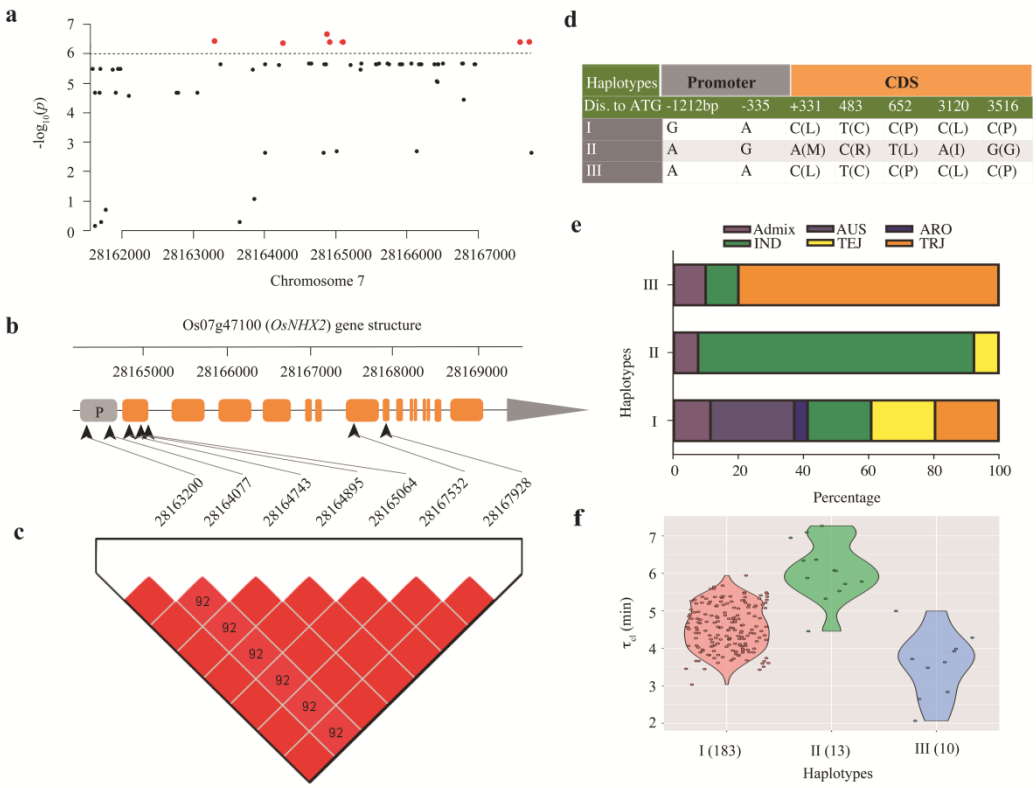

Haplotypes	Promoter		CDS				
Dis. to ATG	-1212bp	-335	+331	483	652	3120	3516
I	G	A	C(L)	T(C)	C(P)	C(L)	C(P)
II	A	G	A(M)	C(R)	T(L)	A(I)	G(G)
III	A	A	C(L)	T(C)	C(P)	C(L)	C(P)

tpj_15004_f4.tif

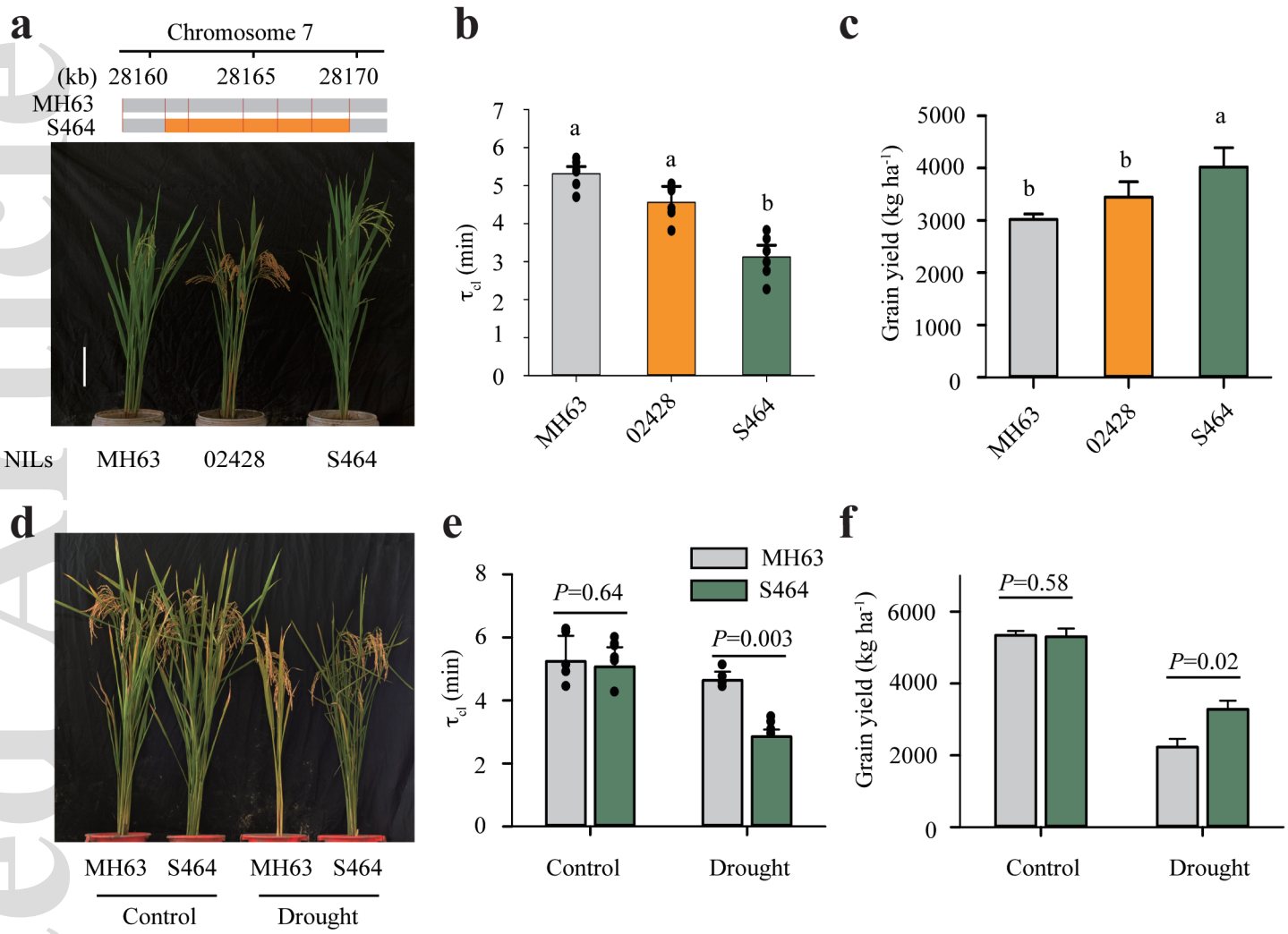

tpj_15004_f5.tif

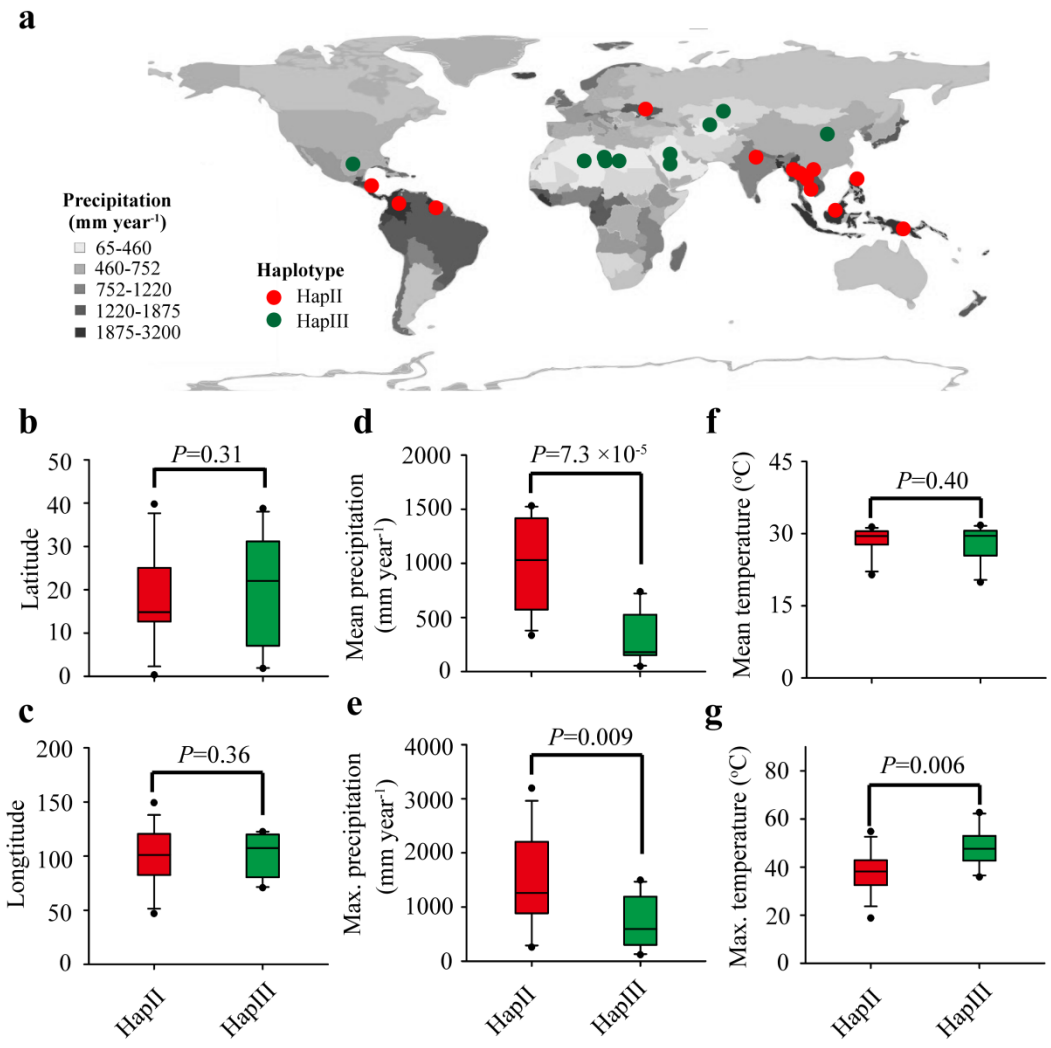

tpj_15004_f6.tif